Preparation and Characterization of Low-Density Polyethylene/Thermoplastic Starch Composites Reinforced by Cellulose Nanofibers

Marzieh Alidadi-Shamsabadi, Tayebeh Behzad, Ruhollah Bagheri, Bijan Nari-Nasrabadi
Department of Chemical Engineering, Isfahan University of Technology, Isfahan, Iran

In the current study, the effect of extracted cellulose nanofibers (CNFs) on rheological and mechanical properties and biodegradability of polyethylene/starch blend was investigated. The CNFs were extracted from wheat straws using a chemo-mechanical method. Polyethylene/starch blend was reinforced by different amounts of CNF (6–14 wt%) using an internal mixer followed by a single screw extruder. The flow properties of nanocomposites were investigated by determining Melt Flow Index (MFI) and viscosity. Due to the weak interaction of cellulosic nanofibers and polymers, the flow behavior of nanocomposites was undesirable. Tensile tests were performed to evaluate the mechanical performance of nanocomposites. By increasing the CNF content, the tensile strength and elongation at break declined; whereas, the Young's modulus was improved. The biodegradation of cellulose nanocomposites was investigated by water absorption and degradability tests. Both experiments confirmed the progressive effect of cellulose nanofibers on the degradation of the composites. POLYM. COMPOS., 36:2309–2316, 2015. © 2014 Society of Plastics Engineers

INTRODUCTION

Low-density polyethylene (LDPE) is one of the fastest growing commercial thermoplastic materials, and the continuous use of polyethylene plastics in different applications has led to the growing problem of environmental pollution. It is necessary to produce LDPE with higher degradation rate in order to overcome this problem. Thermoplastic starch (TPS) is a widely used biopolymer because of its biodegradability, abundant availability, and low cost [1]. However, LDPE/TPS blends have low mechanical performance because of their different polarity, which leads to a poor miscibility and interfacial adhesion [2]. One way to improve the compatibility in LDPE/TPS blend is to use compatibilizing agents such as LDPE-grafted maleic anhydride (LDPE-*g*-MA), which is capable of forming hydrogen bonds with TPS hydroxyls [2, 3]. Although the degradability of LDPE/TPS/LDPE-*g*-MA film is enhanced, it still has low mechanical properties. A developed solution to improve mechanical performance is the incorporation of bio nanofibers to reinforce the blend and producing biodegradable nanocomposites [4]. Recently; cellulose nanofibers (CNFs) have gained a lot of attention due to their relative high strength, stiffness, and low density. Cellulose, a homopolymer of β-1–4 linked D-anhydro glucopyranose unit, is the main component of cellulose fibers [5]. Generally, cellulose-based nanofibers can be extracted and isolated from different sources including cotton, flax, hemp, wheat, rice, jute, sisal, and wood. Because of their annual renewability, agricultural crops-residues can be valuable sources of natural nanofibers. Therefore, in this work, CNFs were extracted from wheat straw using a chemo-mechanical procedure. Then, they were dispersed in LDPE/TPS/LDPE-*g*-MA blends to manufacture nanocomposites. To investigate the effect of nanofibers in LDPE/TPS/LDPE-*g*-MA blends, rheological, mechanical, and water absorption properties of nanocomposites were studied.

EXPERIMENTAL

Materials

Wheat straws were obtained from local fields. Chemicals used in experiments include sodium hydroxide (NaOH) granules, sodium chlorite ($NaClO_2$) 25 wt%, glucose; calcium carbonate powder ($CaCO_3$), and potassium permanganate flakes (KMnO4) were supplied by Merck, Germany. Xylose was obtained from Alpha Aldrich. Hydrochloric acid (HCl) 37 wt%, sulfuric acid (H_2SO_4) 97 wt% and methanol were bought from Arman Sina and Pars companies, Iran, respectively. LDPE (LF0200) (baggage grade) with a density of 0.921 g/cm^3 and a melt flow index (MFI) of 2.2 g/10 min (at 190°C, 2.16 kg load) was obtained from Bandar Emam Polymer

Correspondence to: B.N. Nasrabadi; e-mail: bijannasr@yahoo.com
DOI 10.1002/pc.23144
Published online in Wiley Online Library (wileyonlinelibrary.com).

Petrochemical, Iran. The cornstarch was supplied from Glucosan, Iran. A coupling agent (LDPE-*g*-MA) containing 2 wt% maleic anhydride was brought from Kimia Bespar Asia, Iran. Glycerol was obtained from Pars, Iran.

NANOFIBER EXTRACTION

Chemical Treatment

A chemical treatment is necessary to remove non-cellulosic materials in order to extract nanofibers with high cellulose content. Chemical purification of cellulose from wheat straws was performed according to the method presented by Bhatnagar [6]. First, wheat straws were soaked in a 17.5 wt% NaOH solution for 2 hrs so that the swell cell walls would swell and assist chemical molecules penetration through the crystalline region of cellulose. Afterward, straws were washed with abundant distilled water, followed by blending for 10 min to obtain pulp. The pulp was then air dried for 24 hrs. The pretreated pulp was hydrolyzed by a 2.03 M HCl solution for 2.14 hrs at $80 \pm 5°C$. The hydrolyzed pulp was washed with distilled water until a neutral pH was obtained. After hydrolysis, the sample was treated with a 2 wt% NaOH solution at $80 \pm 5°C$ for 2 hrs [6, 7]. Dilute alkali treatment of lignocellulose fibers separated the structural linkages between lignin and carbohydrate and removed the lignin. Moreover, the remaining hemicelluloses and pectin, which were not dissolved in acid hydrolysis, were removed in this stage. The kappa number (K) is one of the important parameters in pulping industry, which is related to the bleach ability or the degree of delignification of pulp [8]. By measuring the oxidant demand of the pulp with potassium permanganate (KMnO4), the kappa number was determined to estimate the amount of lignin (Klasson lignin) in the pulp [9] according to the following procedure:

$$\text{klasson lignin}(\%) = 0.13 \times \text{kappa number} \quad (1)$$

$$\text{kappa factor} = [\text{equivalent chlorine}(\text{g}/100\,\text{g pulp})]/[\text{kappa number}] \quad (2)$$

Kappa factor is the key number in paper industry to determine the required amount of oxidant for bleaching. This dimensionless number is always in the range of 0–0.25. By selecting a higher kappa factor, pulp with higher brightness prepared by less bleaching will be obtained [10]. In this research, the selected kappa factor was 0.25. The kappa number of the acid and alkali treated sample was determined by measuring the oxidant demand of the pulp with potassium permanganate ($KMnO_4$) [9] and was found to be 83.1 ± 0.2. Each bleaching agent has a specific equivalent chlorine number. Equivalent chlorine number is defined as an amount of chlorine (g or lb) that has the same oxidizing power as one lb or g of the used bleaching agent [9]. In this work, sodium chlorite ($NaClO_2$) was used as a bleaching agent with an equivalent chlorine of 0.73 [6]. The required amount of sodium chlorite was obtained from the following calculations:

$$\text{Equivalent chlorine} = \text{kappa number} \times \text{kappa factor} = 83.1 \times 0.25 = 20.775\,\text{g}/100\,\text{g pulp}$$

$$\text{Required } NaClO_2 = 20.775/(0.73/100) = 0.25\,\text{g/g pulp}$$

To bleach the pulp, the acid and alkali treated pulp and hot water were mixed in a blue cap with the mass ratio of 1:30 [11]. The mixture was then acidified to pH 2.3 with 10 wt% sulfuric acid. An amount of 0.285 g sodium chlorite per 1 g sample was added to the blue cap. Then, the blue cap was placed in the water bath at 50°C and shaken every 5 min. After 60 min, the pulp was washed with distilled water and then air dried [6]. After bleaching fibers, the kappa number of the dry sample was determined again and obtained to be 8.2 ± 0.1, and therefore, the percentage of the residual lignin were reduced to a negligible amount of about $1.1 \pm 0.01\%$. The bleached sample was employed for the sonication stage.

Mechanical Treatment

After the chemical treatment, the fibrillation of the cellulose pulp from wheat straws was performed according to the method presented by Wenshuai Chen et al. [12]. The chemically purified cellulose fibers extracted from the wheat straw were soaked in distilled water (~1 wt%), and the obtained cellulose suspension was then sonicated for 30 min using an ultrasonic common processor with an output power of 400 W to isolate nanofibers. The ultrasonic fibrillation was carried out in an ice bath to prevent overheating [12, 13].

Nanocomposite Sample Preparation

Starch was dried in a vacuum oven for 24 hrs at 80°C. TPS was prepared by pre-mixing starch with 35 wt% liquid glycerol at room temperature and then stored overnight so that the starch granules would swell. Afterward, TPS was melt-blended using an internal mixer with a volumetric chamber capacity of 40 cm^3 at 140°C with the rotor speed of 60 rpm for 8 min. The mixture was taken out and cooled down to room temperature [3, 4]. Suspensions of CNFs were prepared by sonication in distilled water for 10 min with different weight fractions of nanofibers (0, 6, 8, 9, 10, 11, 12, and 14 wt%) based on the total weight of CNF and TPS/LDPE/LDPE-*g*-MA blend. After dispersing the nanofibers, the suspension was added to TPS and mixed by an internal mixer in 60 rpm for 8 min at room temperature. This suspension was left to dry at room temperature for 2 days and then it was placed in a vacuum oven at 37°C for a week [14]. Afterwards, TPS+CNF was melt-blended with LDPE and LDPE-*g*-MA in a laboratory scale Brabender single-screw extruder

DOI 10.1002/pc

TABLE 1. Different formulations of LDPE-TPS nanocomposites.

Samples code	LDPE (wt%)	TPS (wt%)	PE-*g*-MA (wt%)[a]	CNF (wt%)[b]
blank	75	25	3	0
S6	75	25	3	6
S8	75	25	3	8
S9	75	25	3	9
S10	75	25	3	10
S11	75	25	3	11
S12	75	25	3	12
S14	75	25	3	14

[a]base on LDPE+TPS.
[b]base on LDPE+TPS+LDPE-*g*-MA.

[screw diameter (d) = 19 mm, screw ratio (*L*/*D*) = 25:1]. The screw speed was 60 rpm and the temperature profiles along the extruder barrel were 180, 190, 185, and 190°C (from feed zone to die). The obtained blend was extruded twice to improve the homogeneity of nanocomposites. The samples were called based on their nanofiber content as tabulated in Table 1. Nanocomposite films with different weight fractions of CNF were compression molded using a hydraulic press machine. Pre-heating at 155°C for 6 min was carried out followed by compression with a pressure of 10 MPa for 3 min. All the compression molded sheets ($180 \times 180 \times 1 mm^3$) were cold pressed at a rate of 25°C/min to room temperature.

Characterization of Nanofibers and Nanocomposites

The morphology of the extracted nanofibers was characterized using a scanning electron microscope (SEM). The suspensions of CNFs after the ultrasonic process were oven-dried at 105°C after replacement of the solvent from water to ethanol. The obtained sheets were coated with gold and observed under SEM operating at 15 kV. The SEM images of nanofibers were analyzed to measure their diameters and lengths, and consequently to obtain an approximate distribution of fibers diameter and aspect ratio using an image analyzer program (UTHSCSA Image Tool).

The chemical composition of the untreated, acid, and alkali treated fibers were measured in accordance with the standards of the National Renewable Energy Laboratory by NREL test [15]. In this test, cellulose and hemicellulose are degraded to glucose and xylose, respectively; therefore, the amounts of these materials indicate cellulose and hemicellulose contents in the sample. The percentage of acid soluble and insoluble lignin, ash, glucose, and xylose in the samples can be obtained.

The rheological behavior of the nanocomposites was studied by MFI and viscosity measurements. MFI of nanocomposites was determined using an apparatus (Zwick 4100, Germany) (2.16 kg/190°C) with a capillary die of 8 mm length and 2 mm diameter, according to ASTM D 1238-04 (procedure B) [16]. In addition, the apparent viscosity measurement of nanocomposites was carried out using a capillary rheometer (model HAAKE RV 12) at 190°C, which covered the processing temperature range. The mechanical performance of nanocomposites was analyzed according to the ASTMD 638-03 [17] using a tensometer, model Zwick 1446-60 equipped with a 10 KN cell and a data acquisition system. Dumbbell-shaped specimens (2 mm thickness) of nanocomposites were cut from the compression molded sheets. The samples were placed in the grips of the testing machine and stretched with strain rate of 5 mm/min at room temperature. Five replicates were tested for each sample and the average values of the measured properties were reported.

Tensile fracture surfaces were studied by scanning electron microscopy (SEM). The fracture surfaces were sputter coated with a thin layer of gold to avoid electrical charging.

Water absorption of nanocomposite samples was measured using $3 \times 1 mm^2$ strips of 1 mm thickness according to the ASTM D570-98 method [18]. Before measurements, the samples were dried at 70 scanning electron microscopy (SEM)C for 24 hrs in a vacuum oven and then weighed immediately. Water absorption measurements were carried out by soaking the samples in distilled water. At regular time (3 days), each sample was removed from the container, dried, and subsequently weighed to determine its water absorption. The water absorption (%) was calculated as follows:

$$W_t(\%) = [(W_1 - W_0)/W_0] \times 100 \quad (3)$$

where W_0 and W_1 are the initial weight and the weight at time t, respectively [3, 4].

The nanocomposite specimens with the dimension of $20 \times 50 mm^2$ were buried under soil surface of approximately 10 cm. The pH and temperature of the soil were maintained at 7 and 32 ± 2°C, respectively [19]. The water content of the soil was in the range of 10–20% and the weight change was recorded for 30 days. An average percentage of weight change was recorded from three independently tested samples.

RESULTS AND DISCUSSION

Morphology of Cellulose Nanofibers

The ultrasonicated fibers were well-individualized in nanoscale presented in Fig. 1. All the nanofibers displayed a classical web-like network structure and occurred as very long entangled cellulosic filaments. The diameter distribution of the extracted nanofibers is shown in Fig. 2. The average diameter and aspect ratio were found to be 45 ± 3 nm and about 23–54, respectively. The results indicated that fine nanofibers with a suitable diameter distribution were successfully obtained from wheat straws. Therefore, it can be inferred that ultrasonication power destroyed the intermolecular hydrogen

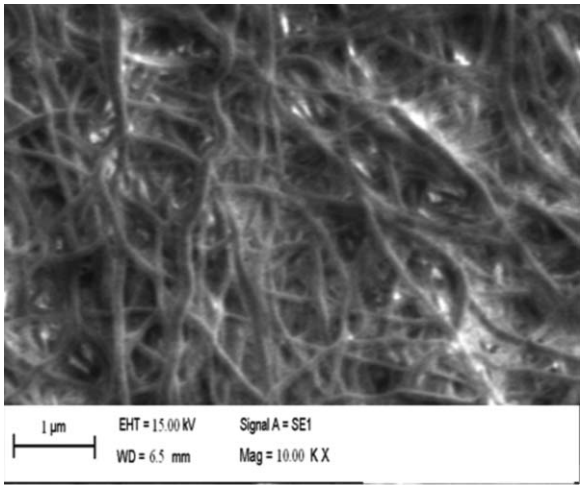

FIG. 1. SEM micrographs of the cellulose nanofibers extracted from wheat straw.

bonds between cellulose chains bundles and strikingly reduced the cellulose fibers dimension to nanoscale.

Chemical Characterization of Nanofibers

The chemical composition of wheat straw fibers before and after chemical treatment (swelling, acid hydrolysis, and alkali treatment) is presented in Table 2. It was found that for the alkali treated fibers (before bleaching), the α-cellulose content (glucose) was increased from 49.8 to 85.5% while hemicellulose (xylose) and total lignin content were significantly decreased to 86 and 53%, respectively. Dilute alkali treatment of lignocellulose fibers separated the structural linkages between lignin and polysaccharides and removed the lignin. In acid hydrolysis, hemicellulose and pectin (amorphous regions) were destroyed and solubilized [7].

Rheological Behavior of the Nanocomposite

Figure 3a shows the variation of MFI values of nanocomposites versus CNF content. The MFI was slightly

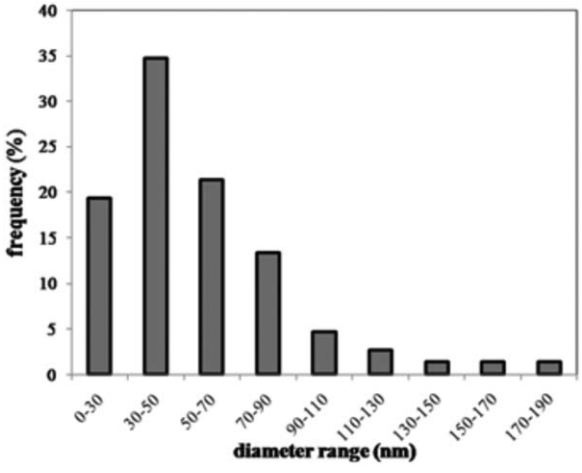

FIG. 2. Diameter distribution of extracted wheat straw nanofibers.

TABLE 2. Chemical composition of the wheat straw fibers (relative % sample).

wheat straw fibers	% Glucose	% Xylose	% Total lignin
Untreated fibers	49.8 ± 0.2	27.2 ± 0.3	23.1 ± 0.1
Acid and alkali treated fibers	85.5 ± 0.5	3.8 ± 0.1	10.8 ± 0.2

reduced by increasing the CNF content from 0 to 10 wt% CNF. The results showed that adding nanofibers decreased the MFI and gave melt stability to LDPE polymer. Therefore, this effect was significantly enhanced by further increasing of CNF content in the matrix (11, 12, and 14 wt%). It can be explained that the use of LDPE-*g*-MA as a compatibilizer in the blends also caused physical and chemical interactions between hydroxyl groups in CNFs surface and anhydride group in LDPE-*g*-MA, which decreased MFI values. In addition, the strong interaction between CNFs caused nanofibers agglomeration, which reduced matrix molecules mobility, and consequently MFI nanocompositeis reduced.

In addition, the apparent viscosity was plotted versus shear rate ($\dot{\gamma}$) of nanocomposites using a logarithmic scale in Fig. 3b. It can be observed that as the shear rate increased from 0.1 to 100 s^{-1}, the apparent viscosity of samples decreased. This confirms that the nanocomposite melts exhibited a shear-thinning behavior since starch degradation rate of amylopectin branches occurred at higher shear rates. The presence of CNFs in composites increased the apparent viscosity at constant shear rate as

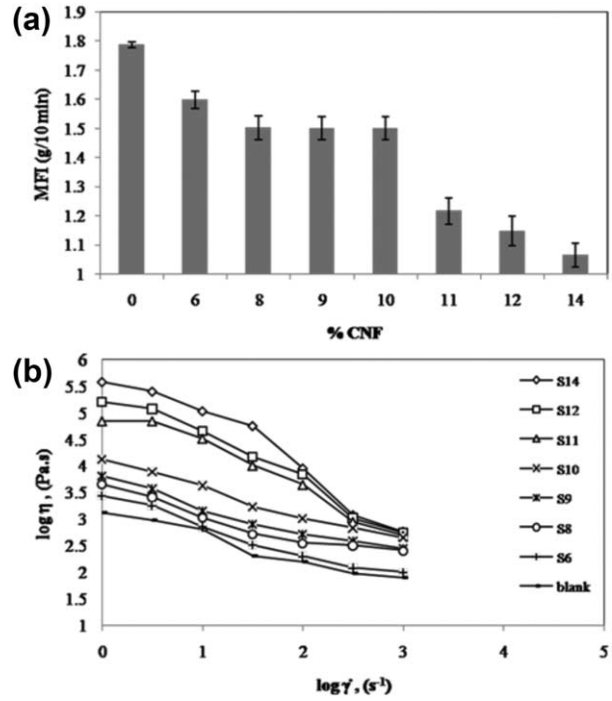

FIG. 3. (a) Melt flow index of nanocomposites versus CNF content. (b) Variation of apparent viscosity versus shear rate of the nanocomposites at different CNF contents.

DOI 10.1002/pc

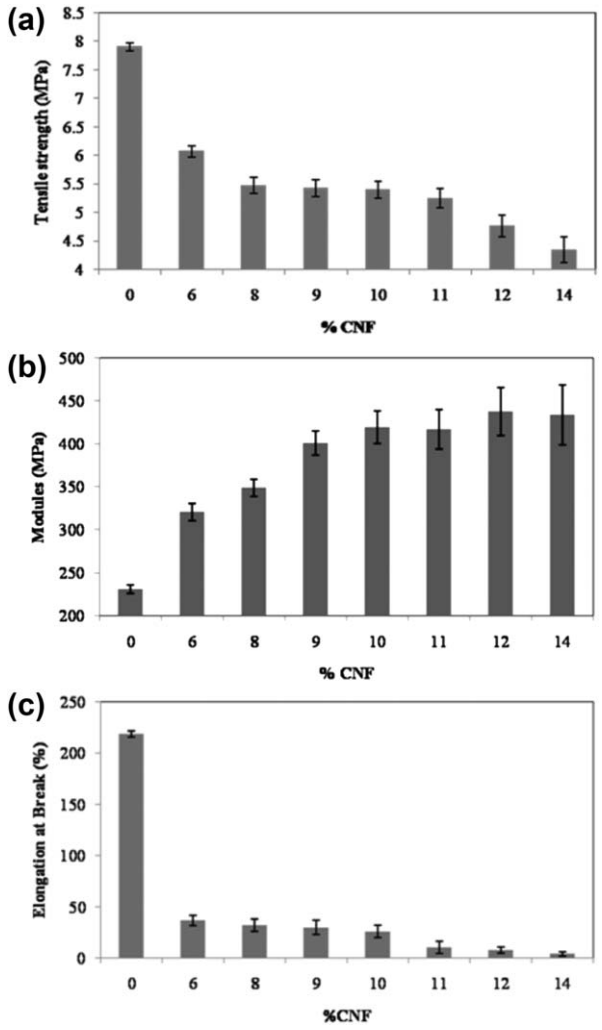

FIG. 4. (a) Tensile strength of nanocomposites versus CNF content. (b) Young's modulus of nanocomposites versus CNF content. (c) Elongation at break of nanocomposites versus CNF content.

compared to the polymer blend (LDPE/LDPE-*g*-MA/TPS). Moreover, by increasing the CNF content, an increase in the apparent viscosity was observed. Addition of CNFs decreases the matrix mobility and consequently would increase the apparent viscosity. It may be caused by the formation of hydrogen bonds between the starch chains, glycerol, and hydroxyl groups of CNFs surface. In addition, the good interaction between anhydride groups in LDPE-*g*-MA and hydroxyl groups of CNFs increased the apparent viscosity of the blends. Difference between apparent viscosities at different CNF contents was more sensible in lower shear rates because of the gradual reduction of physical bonds such as hydrogen bonds.

Tensile Properties of Nanocomposite

Tensile properties of nanocomposites were measured using tensometer. Figure 4a shows variation of the tensile strength versus CNF content. There was a significant reduction in the strength by adding nanofibers (6 wt%) to pure polymer blend. Afterwards, by increasing the CNF content from 8 to 11 wt% no significant changes were observed. In the nanofibers extraction, the swelling stage removed most of wax and oil from the surface so fibers became more hydrophilic [20], whereas the polymer blend is hydrophobic, and this caused a weak interaction between two phases, which decreased the stress transfer through the matrix. Also, the CNFs consisted very high surface area (100 m^2/g), so, possibility of small cracks formations on the surface was higher by adding more CNF [21]. Another challenge was agglomeration of CNFs, which acted as the stress concentrator points and could be intensified by increasing the CNF content. In addition, although adding 3 wt% LDPE-*g*-MA was enough for good interaction of LDPE and TPS, it was not adequate to improve compatibility of LDPE/TPS/LDPE-*g*-MA blend and nanofibers, and therefore, it caused a reduction in the tensile strength. Glycerin decreased adherence between CNFs and matrix, and also diminished the stress transfer from matrix to CNFs (plasticization effect) [22].

Figure 4b shows the effect of CNF content on the Young's modulus of nanocomposites. There was a significant enhancement in the tensile modulus by increasing the CNF content (from 0 to 9 wt%). Since the CNFs have great modulus (140 GPa), which is much higher than LDPE (111 MPa) and TPS (87 MPa) [23, 24] adding nanofibers to the polymer blend has a pronounced effect on the modulus of nanocomposites. However, due to the agglomeration and low dispersion of nanofibers in the matrix, there was a slight increase in the modulus from 10 to 14 wt% nanofibers. The variation of the elongation at break (ε_b) versus CNF content is presented in Fig. 4c. Adding nanofibers significantly reduced the elongation at break. Generally, in synthetic polymers, adding incompatible components to flexible matric limits the motion of polymer chains, and therefore, elongation at break is reduced [5]. However, by increasing the CNF content from 6 to 10 wt%, there was a small reduction in ϵ_b. The interaction between CNFs is stronger than CNF-matrix and therefore, CNFs agglomerate and trap matrix molecules inside their network reduce the matrix molecules mobility. As a result, nanocomposites are ruptured in lower elongation [6]. Also, weak adhesion forces between CNFs and matrix decreased this property. Investigation of the results obtained from the tensile properties suggested that the nanocomposite with 8 wt% nanofibers exhibited the best performance which is in good agreement with the results obtained from other research [25].

Morphology of Composite's Fracture Surface

Figure 5a–c shows the fracture surface of the polymer blend and two nanocomposites (9, 12 wt%). Adding CNFs could cause heterogeneity in the nanocomposites bulk. Weak interfacial interactions between CNFs and the matrix led to form micro cracks in nanocomposites that are shown with arrows in Fig. 5b and c. These micro cracks act as stress concentrated points and reduce the

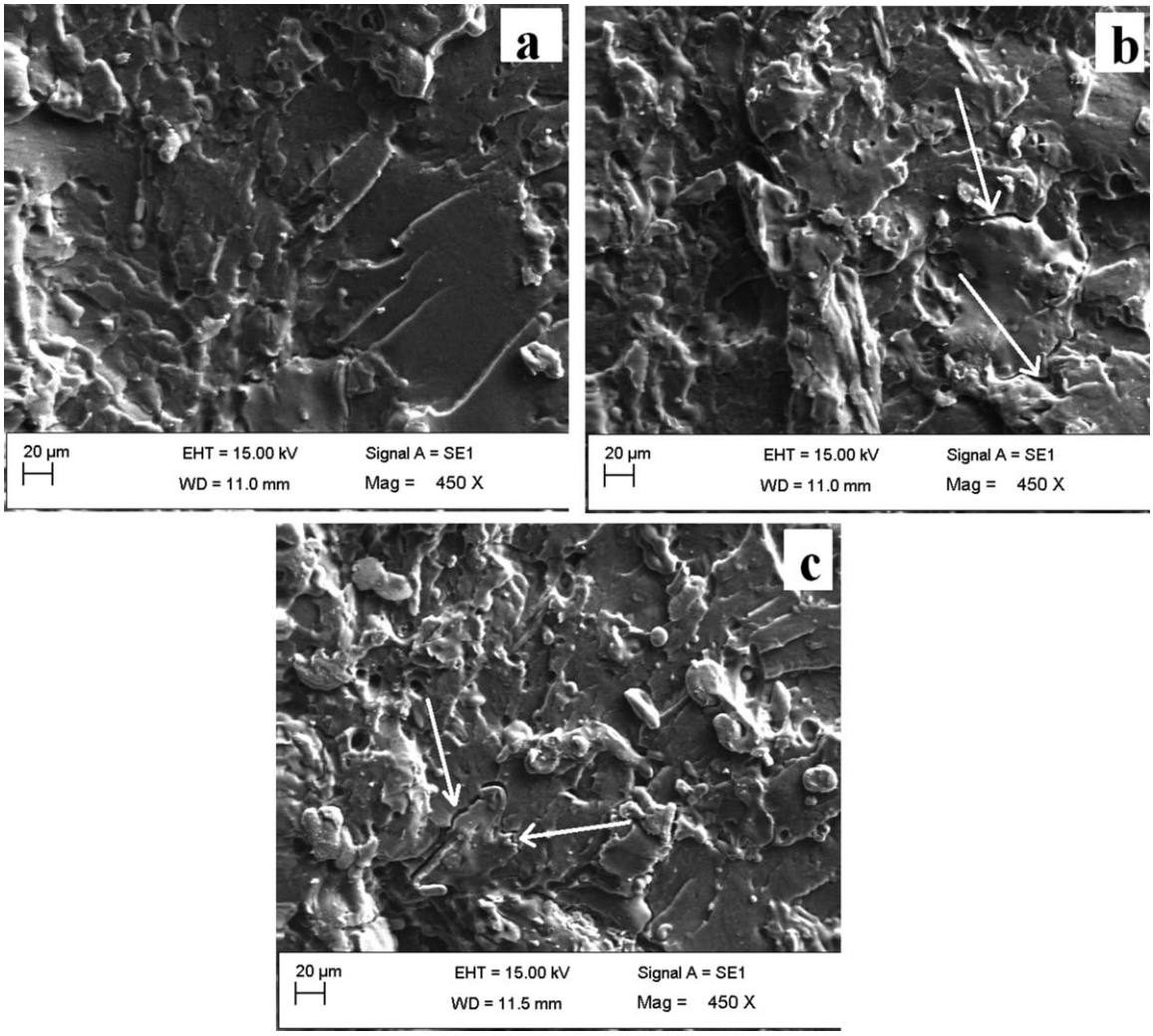

FIG. 5. SEM images of nanocomposites fracture surface (a) 0% CNF, (b) 9% CNF, and (c) 12% CNF.

tensile strength and elongation at the break of nanocomposites.

Water Absorption of Nanocomposite

Figure 6 shows the variation of water absorption versus time for polymer blend and nanocomposites containing various amounts of nanofibers. It can be observed that water absorption was increased with both time of immersion and CNF content. The higher CNF content, the greater water absorption. High water absorption rate was observed for all the samples during the first 6 to 12 days of the immersion time followed by a slow increase. After 24 days, the samples were saturated and achieved a steady state value. Water absorption in first days led to the swelling of porosity, and therefore, cavities walls became thicker and consequently water penetration was limited and the absorption rate was reduced. As it is already known, CNFs have a hydrophilic characteristic while LDPE is very hydrophobic; therefore, increasing the CNF content results in increasing water absorption [19]. Moreover, by increasing the nanofiber content more nanofibers were exposed to the surface of nanocomposites.

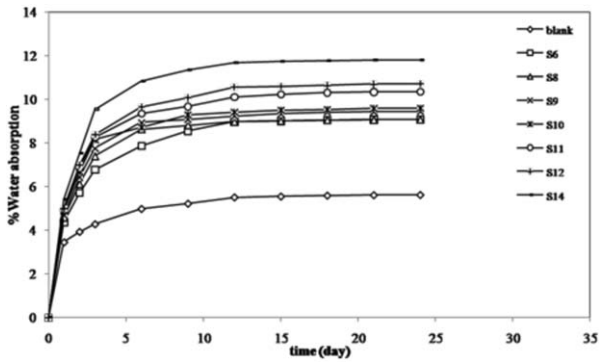

FIG. 6. Water absorption of nanocomposites with different CNF contents versus time.

TABLE 3. Diffusion coefficient for different CNF content.

CNF content (% wt)	0	6	8	9	10	11	12	14
Diffusion coefficient ($\times 10^{-9}$ mm^2/s)	1.53	1.89	2.51	3.05	3.82	5.09	5.41	5.65

DOI 10.1002/pc

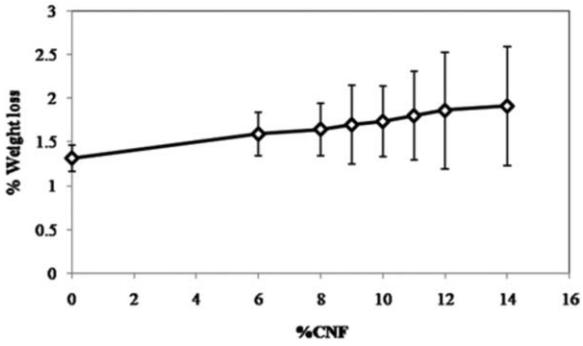

FIG. 7. Weight loss of nanocomposites versus CNF content under soil after 30 days.

Due to the weak interaction between nanofibers and the matrix, small cracks and free volumes were evolved on the surface and the interfacial region of CNF/matrix enhanced water absorption. In addition, anhydride groups of LDPE-*g*-MA react with OH groups of CNFs form ester groups that can result in hydrogen bonding with water [3]. There is an agreement between current results and previous researches on PE-cellulose fibers blend [26].

Diffusion coefficient can be obtained from Fick's second law for plane sheet geometry assuming molecular migration by diffusion and constant diffusion rate and temperature. The equation is as follows:

$$M_t/M_\infty = (4/h)(d/\pi)^{1/2}\, t^{1/2} \quad (4)$$

where M_t and M_∞ are the water uptake of sheet at time t and equilibrium, respectively. The diffusion coefficient and the sample thickness are presented by d and h, respectively. At initial time, i.e., the initial absorption (initial linear portion of the curve) ($M_t/M_\infty \leq 0.5$) [27–29], D can be calculated from the slope of M_t/M_∞ versus $t^{1/2}$. Diffusion coefficients of nanocomposites at different CNF contents are given in Table 3. The diffusion coefficient was increased by increasing the CNF content because of higher hydroxyl group contents.

Degradability of Nanocomposite under Soil

Biodegradable properties of nanocomposites can be determined by the soil burial test. As it can be noticed from Fig. 7, degradation started due to water uptake from the soil, and after 30 days the weight loss was increased for all nanocomposites. The weight loss percentage of the polymers blend was lower than that of nanocomposites since water absorption was higher for nanocomposites because of the hydrophilic nature of TPS and nanofibers. Therefore, adding CNFs to LDPE/TPS blend increased the biodegradability of the blend.

CONCLUSION

In this research, nanocomposites based on LDPE/TPS blend were reinforced by CNFs. CNFs were isolated from wheat straws using a chemo-mechanical method. The chemical purity of the extracted nanofibers was characterized. The average size of nanofibers was obtained to be 45 ± 3 nm. To prepare nanocomposites, first a blend of nanofibers and starch was prepared in an internal mixer, and then the mixture was added to LDPE and LDPE-*g*-MA in a single screw extruder. By increasing the nanofiber content, the tensile strength and elongation at break were decreased because of weak compatibility between CNFs and the matrix. On the other hand, the Young's modulus was improved by increasing CNF content due to high stiffness of CNFs. It was concluded that the most desirable tensile properties were obtained at 8–9 wt% CNF. Due to the agglomeration of nanofibers, MFI of nanocomposites was decreased by increasing the CNF content. Hydrophilic character of CNFs caused higher absorption of water in nanocomposites, which accelerated the biodegradability of LDPE/TPS nanocomposites. The high weight loss of nanocomposites in soil burial test confirmed the higher degradability of nanocomposites with higher nanofiber contents. The obtained results suggested that these nanocomposites as a suitable potential to replace the current non-degradable synthetic products for industry.

REFERENCES

1. H.A. Pushpadass, P. Bhandari, and M.A. Hanna, *Carbohydr. Polym.*, **82**, 1082 (2010).
2. R.A. Majid, H. Ismail, and R.M. Taib, *Polym. Plast. Technol. Eng.*, **48**, 919 (2009).
3. M. Sabetzadeh, R. Bagheri, and M. Masoomi, *J. Appl. Polym. Sci.*, **126**, 63 (2012).
4. J.P. Borges, M.H. Godinho, A.F. Martins, D.F. Stamatialis, M.N. De Pinho, and M.N. Belgacem, *Polym. Compos.*, **25**, 102 (2004).
5. A.P. Kumar and R.P. Singh, *Bioresour. Technol.*, **99**, 8803 (2008).
6. A. Bhatnagar, Isolation *of Cellulose Nanofibers from Renewable Feed Stocks and Root Crops*, Department of Forestry, University of Toronto, Toronto (2004).
7. A. Alemdar and M. Sain, *Bioresour. Technol.*, **99**, 1664 (2008).
8. W. Shen and X. Chen, *Ind. Eng. Chem. Res.*, **48**, 8980 (2009).
9. X.-S. Chai and J.Y. Zhu, U.S. Patent 6,475, 339 (2002).
10. X.S. Chai and J.Y. Zhu, *J. Pulp Pap. Sci.*, **25**, 387, (1999).
11. M.F. Rosa, E.S. Medeiros, J.A. Malmonge, K.S. Gregorski, D.F. Wood, L.H.C. Mattoso, G. Glenn, W.J. Orts, and S.H. Imam, *Carbohydr. Polym.*, **81**, 83 (2010).
12. W. Chen, H. Yu, Y. Liu, P. Chen, M. Zhang, and Y. Hai, *Carbohydr. Polym.*, **83**, 1804 (2011).
13. W. Chen, H. Yu, Y. Liu, Y. Hai, M. Zhang, and P. Chen, *Cellulose*, **18**, 433 (2011).
14. A. Alemdar and M. Sain, *Compos. Sci. Technol.*, **68**, 557 (2008).
15. A. Sluiter, B. Hames, R. Ruiz, C. Scaxlata, J. Sluiter, D. Templeton, and D. Crocker, *Determination of Structural Carbohydrates and Lignin in Biomass*, NREL/TP-510–42618, NREL, National Laboratory of the U.S. (2008).

16. Standard Test Method for Melt Flow Rates of Thermoplastics by Extrusion Plastometer, ASTM/D1238-04, ASTM, U.S. (2004).
17. Standard Test Method for Tensile Properties of Plastics, ASTM/D638-03, ASTM, U.S. (2004).
18. Standard Test Method for Water Absorption of Plastics, ASTM/D570-98, ASTM, U.S. (2004).
19. J. Prachayawarakorn, P. Sangnitidej, and P. Boonpasith, *Carbohydr. Polym*., **81**, 425 (2010).
20. X. Li, L.G. Tabil, and S. Panigrahi, *J. Polym. Environ*., **15**, 25 (2007).
21. Y. Chen, C. Liu, P.R. Chang, X. Cao, and D.P. Anderson, *Carbohydr. Polym*., **76**, 607 (2009).
22. L. Avérous and P.J. Halley, *Biofuels, Bioprod. Biorefin*., **3**, 329 (2009).
23. H. Takagi and A. Asano, *Compos. Part A*, **39**, 685 (2008).
24. L. Averous, C. Fringant, and L. Moro, *Polym. J*., **42**, 6565 (2001).
25. A. Junior de Menezes, G. Siqueira, A.A.S. Curvelo, and A. Dufresne, *Polym. J*., **50**, 4552 (2009).
26. C.S.R. Freire, A.J.D. Silvestre, C.P. Neto, A. Gandini, L. Martin, and I. Mondragon, *Compos. Sci. Technol*., **68**, 3358, (2008).
27. A. Kaushik, M. Singh, and G. Verma, *Carbohydr. Polym*., **82**, 337 (2010).
28. A. Dufresne, D. Dupeyre, and M.R. Vignon, *J. Appl. Polym. Sci*., **76**, 2080 (2000).
29. Y.Z. Wan, H. Luo, F. He, H. Liang, Y. Huang, and X.L. Li, *Compos. Sci. Technol*., **69**, 1212 (2009).

DOI 10.1002/pc